Transmitter-in-the-Loop Optimization of Distorted OFDM Radar Emissions

John Jakabosky[1], Lane Ryan[1,2], and Shannon Blunt[1]
[1] Radar Systems Lab, University of Kansas, Lawrence, KS
[2] Honeywell FM&T, Kansas City, MO

***Abstract*—The inherent amplitude modulation of orthogonal frequency division multiplexing (OFDM) has limited its use in radar due to transmitter-induced distortion. Specifically, there is a necessary trade-off between reduced SNR caused by power back-off to accommodate these AM effects and the waveform distortion that occurs when driving the amplifier closer to saturation. Here a method is developed to design OFDM-based radar emissions with low range sidelobes in the presence of transmitter-induced distortion. This work builds upon previous results for hardware-in-the-loop optimization of continuous phase modulation (CPM) waveforms to demonstrate how saturated OFDM emissions may potentially provide a feasible alternative waveform design scheme.**

I. Introduction

The development of a radar system involves numerous physical constraints and design trade-offs according to myriad factors such as the desired operating modes, expected conditions of the operating environment, and deployment and maintenance costs. As such, the conventional "divide and conquer" approach is used to design each individual component according to a set of specifications that will ensure some nominal level of performance for the overall system. However, from an optimization theory perspective this component-centric design strategy clearly limits the capability of the radar by forcing multiple locally optimal choices. In contrast, here we shall examine one of many possible facets for holistic radar design by optimizing the resulting physical emission produced from driving an OFDM-based radar waveform into a distortion-inducing power amplifier.

It has recently been demonstrated [1,2] that continuous phase modulation (CPM) based waveforms can be optimized for radar with a design goal of low range sidelobes. CPM-based waveforms have the intrinsic benefit of a 0 dB peak-to-average-power ratio (PAPR) that provides a high level of power efficiency and natural resilience to amplifier-induced distortion. Here it is shown that a similar approach can be taken for transmitter-distorted OFDM-based emissions, thereby facilitating use of different design degrees of freedom.

The OFDM modulation scheme is widely used in communications and serves as the basis for Fourth Generation (4G) commercial standards such as WiMAX and LTE [3]. More recently, OFDM has been examined as an alternative framework for radar waveform design [4-7], as a way to unify communication and radar emission [8], and as the basis for passive sensing via exploitation of WiFi emissions [9].

An OFDM signal is constructed in the frequency domain; thus control of the spectrum can be directly obtained. Unlike traditional radar waveforms, however, OFDM is not constant modulus (PAPR > 0 dB). In fact, the peak power of an OFDM waveform may far exceed the average power, which presents a trade-off problem for its use in radar. The intrinsic amplitude modulation (AM) of OFDM requires linear amplification to avoid compression of the higher amplitude components and a subsequent distortion-induced increase in range sidelobes. However, linear amplification means the radar could be emitting far below the maximum output power, which limits power efficiency and "energy on target", thus hindering detection performance. To circumvent this trade-off we consider optimization of the distorted OFDM emission after the effects of amplifier compression.

The optimization method used in [1,2] to design CPM-based radar waveforms will here be leveraged to design transmitter-distorted OFDM radar waveforms. This method employs a greedy search for discrete optimization problems and has been shown to be effective for high dimensionality [10]. However, the CPM framework in [1,2] employed a constant-modulus PSK symbol constellation so that optimization of the CPM-based waveform was performed on a one-dimensional search space (i.e. phase). In contrast, for OFDM the quadrature amplitude (QAM) constellation is used thereby necessitating a two-dimensional search space (over the I and Q amplitude components) for OFDM-based radar waveforms. The following outlines the basic structure for OFDM.

II. OFDM Radar Implementation

We consider an OFDM waveform that occupies what would otherwise be a single symbol interval (though is easily extensible to multiple symbol intervals) and is modulated onto a rectangular pulse shape. For simplicity, the signal is represented at baseband. The OFDM waveform can be expressed as

$$s(t) = \sum_{n=1}^{N} d_n \exp(j2\pi f_n t) \tag{1}$$

where the values for d_n are symbols taken from a QAM constellation of arbitrary size, the subcarrier frequencies are

This work was supported by the Radar Division of the US Naval Research Laboratory under contract N-00173-12-P-0998.

$$f_n = \frac{n}{N} B \ , \tag{2}$$

with N the number of subcarriers. The pulse width is $T = N/B$ for B the bandwidth of the waveform. Thus the time-bandwidth product is $TB = N$. The collection of the N symbols is defined as the vector $\mathbf{d}$ which corresponds to the OFDM version of a radar code (albeit one defined in the frequency domain).

In general, the OFDM waveform in (1) can possess significant amplitude modulation. To prepare the OFDM waveform for injection into the power amplifier, the amplitude of the waveform is first clipped by a limiter to balance between linearity and average power. The rule used here for clipping is

$$|s_c(t)| = \begin{cases} \sqrt{LP_A}, & \text{if } |s(t)| > \sqrt{LP_A} \\ |s(t)|, & \text{otherwise} \end{cases} \tag{3}$$

where P_A is the average power of the original waveform and L is the peak power of the limiter. This approach has the effect of limiting PAPR through intentional pre-distortion, which is necessary due to the maximum input drive level that can be tolerated by the power amplifier without damaging it. The resulting clipped waveform is thus

$$s_c(t) = |s_c(t)| e^{j\angle s(t)} \tag{4}$$

where $\angle s(t)$ indicates the phase of the original (unclipped) waveform.

To represent the performance of an OFDM emission fully, the distortion of the power amplifier must be considered. To maximize the power efficiency, it is desired to operate the power amplifier in saturation, which produces nonlinear compression. Letting $T[\bullet]$ be the operation representing distortion by the transmitter, the final emission is therefore

$$e(t) = T[s_c(t)] . \tag{5}$$

This nonlinear distortion was shown in [2] to cause an increase in range sidelobes for CPM-based waveforms. It is expected that an OFDM waveform will be more susceptible to this source of sidelobe degradation due to its inherent amplitude modulation. Thus it is the physical emission $e(t)$ from (5) that we shall optimize.

III. Emission Optimization

The QAM constellation associated with each d_n value consists of K symbols on a square lattice in the complex I-Q plane. Each of the N subcarriers is modulated by one of these symbols thus resulting in N^K possible radar waveforms. To search this high dimensional solution space the greedy optimization approach described in [1,2] is employed.

Given an initial set of symbols for the N subcarriers, the optimization strategy operates by selecting which of the K symbols yields the best performance improvement for a given subcarrier in terms of the range sidelobes of the physical emission $e(t)$. Subsequently, the symbol providing the most improvement for a different subcarrier is selected. This process is repeated for each of the subcarriers until no further improvement can be found. The ordering of the subcarriers may be arbitrary or ranked according to the maximum performance improvement over all N at each stage of optimization.

The quality of the emission is evaluated according to the sidelobe level of the autocorrelation of $e(t)$. This measure of quality could be either integrated sidelobe level (ISL), peak sidelobe level (PSL), or some other appropriate metric. Here PSL is used.

The optimization of the OFDM emission for transmitter effects can be performed using a mathematical model of the transmitter, denoted as Model-in-the-Loop (MiLo), or using the actual physical hardware, denoted as Hardware-in-the-Loop (HiLo). A diagram of this holistic optimization scheme is shown in Figure 1.

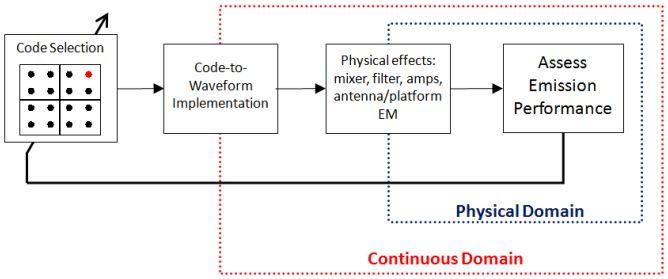

Figure 1. Transmitter-in-the-loop optimization of OFDM waveforms

A. Model-in-the-Loop (MiLo) Optimization

The MiLo approach uses a mathematical transmitter model [11] comprised of a band-limiting filter $h(t)$ and a saturated power amplifier model. The filter produces $\tilde{\ }$ $) * s_c(t)$ and the subsequent power amplifier model yields

$$e(t) = \tilde{\ } \quad \tilde{\ } \ , \tag{6}$$

where the compression term $G[\bullet$ is defined as

$$G[r] \triangleq \frac{A(|r|)}{|r|} \tag{7}$$

and

$$A(r) = \frac{vr}{\left[1 + \left(\frac{vr}{A_0}\right)^{2p}\right]^{1/2p}} \ . \tag{8}$$

The value p in (8) determines the softness of transition from the linear to non-linear operation of the amplifier, A_o is the saturating output amplitude, and v is the small signal gain.

B. *Hardware-in-the-Loop (HiLo) Optimization*

Optimization for the Hardware-in-the-loop case is performed on a radar test bed (see Fig. 2). The OFDM waveform is generated in software, uploaded to an arbitrary waveform generator, injected through a transmitter/receiver pair, and then sampled by a digitizer. The PSL of the sampled "received" emission is ascertained to drive the optimization process.

Here the transmitter is comprised of a class A power amplifier operated in saturation. The output of the transmitter is immediately attenuated and connected via loopback directly into the receiver. The power level of the input to the receiver is kept well below the compression point to avoid receiver-induced nonlinearities. Free-space HiLo optimization within an anechoic chamber is planned for the near future.

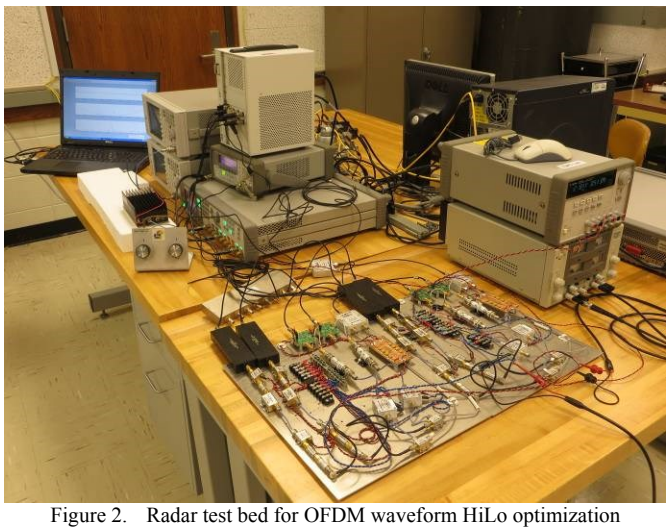

Figure 2. Radar test bed for OFDM waveform HiLo optimization

IV. Simulation & Experimental Results

Here we consider the efficacy of optimizing a transmitter-distorted OFDM radar emission. To initialize the search process, a code having $N = 64$ subcarriers (so $BT = 64$) was randomly populated such that each subcarrier is assigned a symbol from the QAM-64 constellation (8×8 in the *I-Q* plane). Thus $K = 64$ and there are 2^{384} possible waveforms (making full enumeration of all possibilities infeasible). The waveform bandwidth was set to 40 MHz and the receiver sampling rate to 1 GHz. The clipping value was set to $\sqrt{LP_A} = 2$.

First an idealistic OFDM waveform that is free of clipping or distortion was optimized using the greedy search approach. The performance of the optimized OFDM waveform under idealized conditions is shown in Table 1 under "Ideal". For this idealistic case, depicted as the black trace in Figures 3-7, the peak sidelobe level (PSL) was found to be −29.7 dB and the integrated sidelobe level (ISL) to be −14.5 dB.

A. *Model-in-the-Loop Optimization*

The idealistic OFDM waveform was injected through the transmitter model from Sect. III.A using the model values v=10, A_o=1, and p=3. The performance of the resulting distorted emission is shown in Table 1 under the "MiLo" heading. Due predominantly to compression of the AM characteristics of the idealistic OFDM waveform, the MiLo emission experiences a PSL degradation of 14.7 dB and an ISL degradation of 11.7 dB.

The optimization procedure was then repeated with the modeled distortion in the loop. The results of this second optimization are shown in Table 1 under the heading "MiLo-opt" where nearly all of the idealized performance is regained. Specifically, the PSL value is reduced to within 1.9 dB of the idealistic case and the ISL value is reduced to within 2.0 dB of ideal ("Δ Ideal" column in Table1). The two MiLo emissions are compared to the idealistic waveform in Figures 3 and 4.

The amplitude compression effect of the modeled power amplifier is illustrated in Fig. 5. The amplitude compression can be viewed as a forcing of the emission towards constant modulus. This effect is also realized by the reduction of the 8.6 dB PAPR value for the idealistic waveform to 0.3 dB and 1.2 dB for the MiLo and MiLo-opt cases emissions, respectively. It is interesting to note that the MiLo optimization produced a PAPR increase from 0.3 to 1.2 dB, implying that some amplitude modulation is useful from the perspective of design degrees-of-freedom.

Table 1. MiLo Emission comparison in dB

	Ideal	**MiLo**	**MiLo-opt**	**Δ Ideal**
PSL	−29.7	−15.0	−27.8	1.9
ISL	−14.5	−2.8	−12.5	2.0
PAPR	8.6	0.3	1.2	−7.4

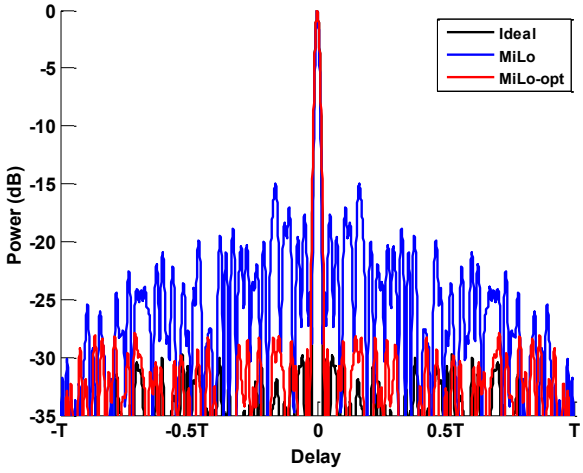

Figure 3. Comparison of Ideal and MiLo Autocorrelations

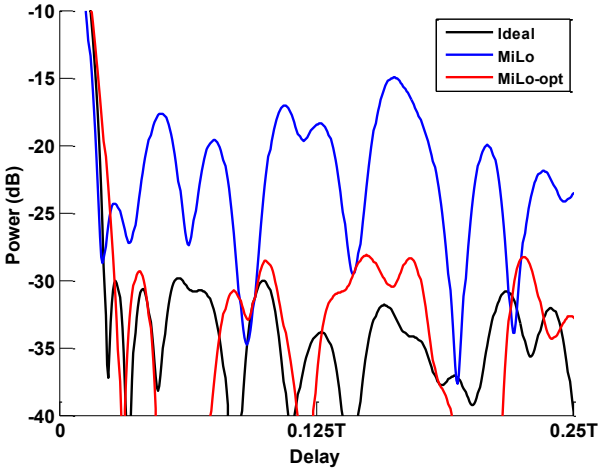

Figure 4. Comparison of Ideal and MiLo (close up)

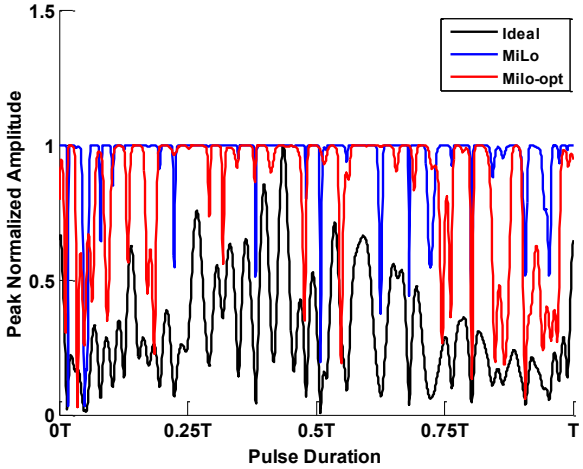

Figure 5. Amplitude of Ideal and MiLo Emissions

B. *Hardware-in-the-Loop Optimization*

Finally, the idealistic waveform was injected into the physical hardware of the radar test bed and the performance of the output emission evaluated. The Class A power amplifier was operated in saturation (5 dB beyond the 1 dB compression point). The result of transmitter distortion upon the ideal emission is shown in Table 2 under the "HiLo" heading. The HiLo distortion yielded a PSL degradation of 11.5 dB and an ISL degradation of 5.4 dB. The PAPR was reduced to 4.8 dB. Note that the PSL and ISL degradation was worse in the MiLo case than observed here because the latter was used to model a power amplifier with more severe distortion. A comparison of the PAPR reduction for the two cases verifies that effect.

Hardware-in-the-loop optimization was then applied to the transmitter-distorted emission to determine how much of the degradation from the idealistic case could be recovered. The results of this optimization are shown in Table 2 under the heading "Hilo-opt". The PSL value was decreased to within 2.2 dB of the idealistic case. The ISL was reduced to be within 2.9 dB of ideal. No change in PAPR from the HiLo case occurred. The values of ISL and PSL for the optimized HiLo case are comparable to those from the optimized Milo case. The HiLo and optimized HiLo emissions are compared to the idealistic waveform in Figs. 6 and 7.

Table 2. HiLo Emission comparison in dB

	Ideal	HiLo	HiLo-opt	Δ Ideal
PSL	−29.7	−18.3	−27.5	2.2
ISL	−14.5	−9.4	−11.6	2.9
PAPR	8.6	4.8	4.8	−3.8

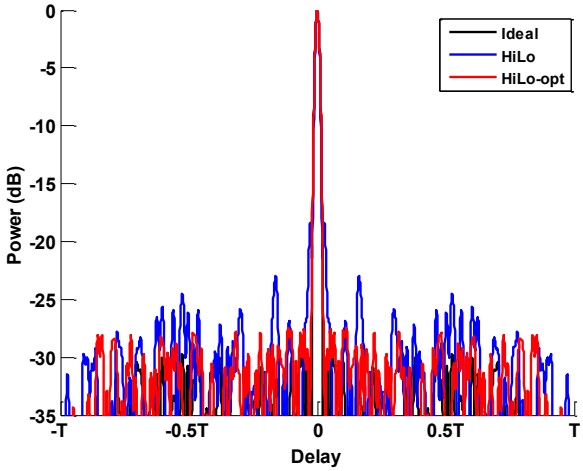

Figure 6. Comparison of Ideal and HiLo Autocorrelations

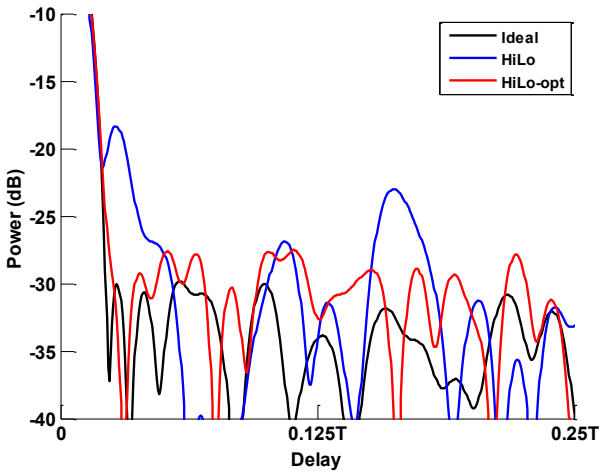

Figure 7. Comparison of Ideal and HiLo (close up)

C. *Delay-Doppler Ambiguity*

The delay-Doppler ambiguity functions for the ideal, optimized MiLo ('MiLo-opt'), and optimized MiLo ('HiLo-opt') emissions are shown in Figs. 9, 10 and 11, respectively. As expected, all three emissions realize a thumbtack-like response with higher sidelobes away from the zero-Doppler cut. Because the optimization strategy is amenable to incorporating non-zero Doppler into the assessment process, future work will examine how Doppler tolerance, generally

considered to be obtainable only by waveforms close to a linear chirp, may be generated from the OFDM framework.

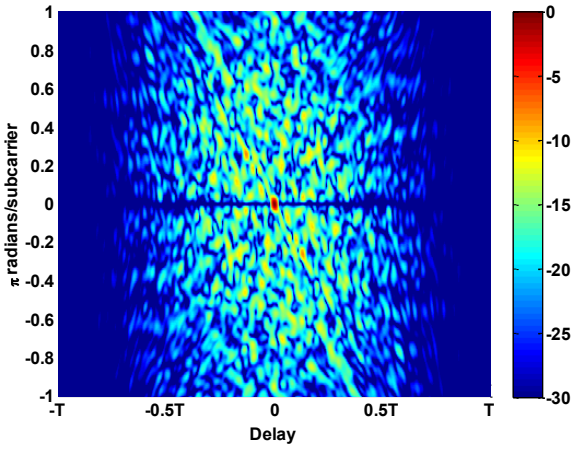

Figure 8. Delay -Doppler ambiguity of the Ideal optimized emission

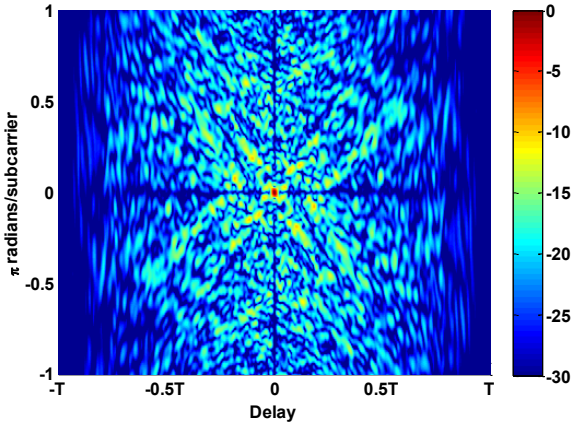

Figure 9. Delay -Doppler ambiguity of the MiLo optimized emission

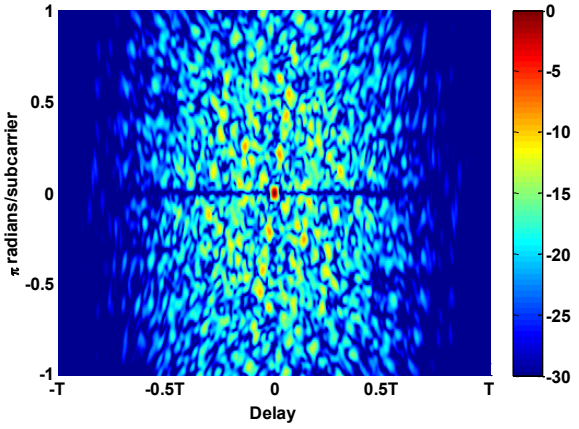

Figure 10. Delay-Doppler ambiguity of the HiLo optimized emission

CONCLUSIONS

A method for optimizing transmitter-distorted OFDM emissions was presented. An ideal OFDM waveform was generated that exhibited a PSL of −29.7 dB with 64 subcarriers for a single symbol interval. The waveform was non-linearly distorted by a radar transmitter. The transmit hardware was represented by a modeled amplifier and by a radar testbed that included a saturated power amplifier. The same optimization approach was used to compensate for distortion induced by the modeled and physical transmit hardware. The model-optimized emission yielded a PSL of −27.8 dB while the hardware-optimized emission resulted in a PSL of −27.5 dB. The optimization was capable of recovering nearly all of the degradation introduced by the transmitter. Furthermore, the optimized waveforms were shown to maintain a similar thumbtack-like delay-Doppler ambiguity function. The use of the optimization approach to reduce Doppler sidelobes and PAPR are topics of further study.

REFERENCES

[1] J. Jakabosky, P. Anglin, M.R. Cook, S.D. Blunt, and J. Stiles, "Non-linear FM waveform design using marginal Fisher's information within the CPM framework," *IEEE Radar Conference*, Kansas City, MO, pp. 513-518, May 2011.

[2] J. Jakabosky, S.D. Blunt, M.R. Cook, J. Stiles, and S.A. Seguin, "Transmitter-in-the-loop optimization of physical radar emissions," *IEEE Radar Conference*, Atlanta, GA, pp. 874-879, May 2012.

[3] M. Ergen, *Mobile Broadband – Including WiMAX and LTE*, Springer, 2009.

[4] N. Levanon and Mozeson, *Radar Signals*, John Wiley & Sons, 2004, Chap. 11.

[5] S. Sen, G. Tang, and A. Nehorai, "Multiobjective optimization of OFDM radar waveform for target detection," *IEEE Trans. Signal Processing*, vol. 59, no. 2, pp. 639-652, Feb. 2011.

[6] R.F. Tigrek, W.J.A. De Heij, and P. Van Genderen, "OFDM signals as the radar waveform to solve Doppler ambiguity," *IEEE Trans. Aerospace & Electronic Systems*, vol. 48, no. 1, pp. 130-143, Jan. 2012.

[7] R. Mohseni, A. Sheikhi, and M.A.M Shirazi, "Constant envelope OFDM signals for radar applications," *IEEE Radar Conference*, Rome, Italy, May 2008.

[8] C. Sturm and W. Wiesbeck, "Waveform design and signal processing aspects for fusion of wireless communications and radar sensing," *Proc. IEEE*, vol. 99, no. 7, pp. 1236-1259, July 2011.

[9] F. Colone, P. Falcone, C. Bongioanni, and P. Lombardo, "WiFi-based passive bistatic radar: data processing schemes and experimental results," *IEEE Trans. Aerospace & Electronic Systems*, vol. 48, no. 2, pp. 1061-1079, Apr. 2012.

[10] J.D. Jenshak and J.M. Stiles, "A fast method for designing optimal transmit codes for radar," *IEEE Radar Conference*, Rome, Italy, May 2008.

[11] E. Costa, M. Midrio, and S. Pupolin, "Impact of amplifier nonlinearities on OFDM transmission system performance," *IEEE Communications Letters,* vol. 3, no. 2, pp. 37-39, Feb. 1999.